Samara State Aerospace University

D.A. Uglanov

Supersonic flow in channel of variable section and around the circle cylinder

methodology instructions for laboratory works

Samara, 2014

Contents

Chapter 1. Supersonic flow in the channel with variable section

The purpose of the work is to determine experimentally the change of the static parameters and air motion velocity along the flow in plane supersonic nozzle on non-design regime with overexpansion and to determine the location of the shock wave inside the nozzle.

1.1 Theoretical basis of the experiment

In the supersonic nozzle, which is called Laval nozzle, gas flow transform in such way that discharge velocity became larger than speed of sound a, i.e. $c > a$, $M > 1$, where $M = \frac{c}{a}$ - relative gas motion velocity,

$$a = \sqrt{\kappa RT} = \sqrt{k\frac{p}{\rho}} = \sqrt{\frac{dp}{d\rho}}; \quad (1.1)$$

Let's consider continuity and energy equations for steady gas motion in differential form without heat and hydraulic losses, i.e. during gas condition change by ideal adiabatic law

$$d(\rho,c,S) = 0, \quad (1.2)$$

$$dp+\rho cdc = 0, \quad (1.3)$$

where ρ – gas density,

c – discharge velocity,

S – section area,

p – gas static pressure.

After conversation and joint solution of the (2) and (3) equations with taking (1) into account, we get:

$$\left(\frac{c^2}{a^2}-1\right)\frac{dc}{c} = \frac{dS}{S} \quad (1.4)$$

Analyzing this equation, we get:

if $c < a$, $\frac{dS}{S} < 0$ (narrowing),

if $c = a$, $\frac{dS}{S} = 0$ (crisis),

if $c > a$, $\frac{dS}{S} > 0$ (expansion).

Thus, three regimes of gas flow exist: subsonic ($c < a_{cr}$), critical ($c = c_{cr} = a_{cr}$) and supersonic ($c > a_{cr}$).

Supersonic flow suited for supersonic flow creation consists of narrowing (subsonic) and expansion (supersonic) parts (fig. 1).

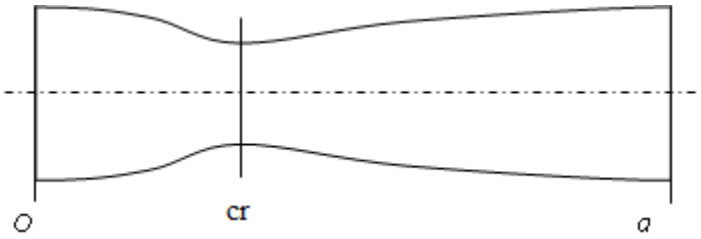

Fig. 1.1. Supersonic (Laval) nozzle

In most narrow flow section (critical section) gas velocity is equal to local speed of sound.

Gas parameters in critical sections are called critical parameters and that's why

$$c = c_{кр},\ a = a_{кр}\ u\ c_{кр} = a_{кр} = \sqrt{\frac{2\kappa}{\kappa + 1} RT}^{*} \qquad (1.5)$$

If gas is considered ideal, critical section correlate with minimal nozzle section, i.e. $S_{cr} = S_{min}$.

During the viscous gas flow, boundary layer, caused by the flow deceleration near rough walls, take place. The influence of this boundary layer leads to displacement of the flow critical section to expansive part of the supersonic flow. If thickness of the boundary layer is small relatively to flow section area, critical section is assumed equal to minimal section even during real gas flow.

On design regime of the supersonic nozzle, pressure p_a in the gas flow on the exit section of the nozzle is equal to the pressure of the environment which is called negative pressure p_{neg}, i.e. $p_a = p_{np}$.On this regime, continuous decreasing of the static pressure, temperature, gas density and velocity increasing along the axis of its motion in direction to the flow takes place.

Gas discharge from the nozzle velocity (fig. 1.1, sec. a) on design regime has maximum value

$$c_{cp} = \sqrt{\frac{2\kappa}{\kappa+1} RT^* \left[1 - \left(\frac{p}{p^*_{cp}}\right)^{\frac{\kappa-1}{\kappa}}\right]}. \qquad (1.6)$$

In case of energetically insulated gas flow, i.e. if $l_{мех} = 0$; $q_н = 0$, stagnation temperature T^* in the supersonic nozzle remains constant in all flow area inside the nozzle either for ideal or for real gases, i.e. $T^* = const$. Stagnation pressure p^* is constant only in case of ideal (non-viscous) gas. In nozzles with real gas stagnation pressure p^* decreases. Stagnation pressure changing is estimated by convention by the $\sigma = \frac{p^*_i}{p^*_0}$ coefficient, where p^*_i, p^*_0 are stagnation pressures correspondingly in arbitrary i and initial 0 flow sections.

If $p_{neg} \neq p_a$ during the gas discharge from the supersonic nozzle, nozzle operating regime is called non-design. If $p_{neg} < p_a$, non-design regime with underexpansion takes place, and if $p_{neg} > p_a$, non-design regime with overexpansion takes place.

Important feature of the gas flow in the Laval nozzle is that, if $p_{np} / p_a < (2{,}0 \ldots 3{,}0)$, gas flow inside the nozzle on all regime is the same as on corresponding design regime. Herewith, $p_a = p_{a(des)}$ and it is obviously can be $p_a \leq p_{neg}$ (fig. 1.2,sec. a).

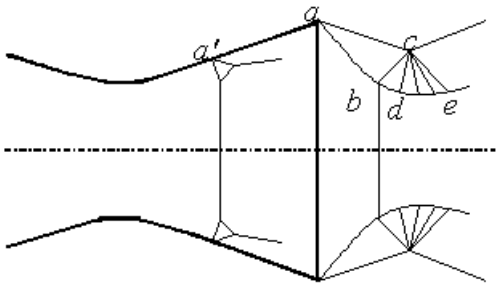

Fig. 1.2. Discharge from the Laval nozzle with strong overexpansion, abc – is bridging shock wave on the exit section, a' – shock wave inside the nozzle which causes flow separation.

If supersonic nozzle operates with high negative pressures, when $p_{пр} / p_{а(расч)} > (2{,}0 \ldots 3{,}0)$, complicated system of the shock waves, which can be approximately considered as direct shock wave, appears in gas flow inside the nozzle.

Before the shock wave gas parameters change as in the supersonic nozzle on design regime: in the shock wave itself static pressure p, temperature T and density ρ abruptly increase and velocity c and stagnation pressure p^* decrease.

Stagnation pressure in section after the direct shock wave is determined with $\sigma_{d.s.w}$ coefficient:

$$p^*_{aft} = p^*_{bef} \cdot \sigma_{d.s.w} = p^*_{bef} \cdot \lambda^2_{bef} \cdot \left[\frac{1 - \frac{\kappa - 1}{\kappa + 1} \lambda^2_{bef}}{1 - \frac{\kappa - 1}{\kappa + 1} \cdot \frac{1}{\lambda^2_{bef}}} \right]^{\frac{1}{\kappa - 1}}, \qquad (1.7)$$

where $\lambda_{bef} = \frac{c_{bef}}{a_{cr}}$ is relative velocity in the section before the shock wave.

After the shock wave, gas flow parameters vary as in the subsonic diffuser, i.e. static pressure, temperature and density increase and velocity decrease because flow after the direct shock wave became subsonic.

The reality is that gas parameters in the shock wave are changing under interaction with boundary layer not in the one section but in some layer of gas, which has finite thickness, i.e. shock wave is stretched along the gas flow.

With increase of $p_{neg}/(p_a)_{calc}$ the flow in “narrow” section of the nozzle and, consequently, along all nozzle length became subsonic. On that regime channel of variable section (fig. 1.1), where subsonic flow takes place, is called Venturi tube and doesn’t represent supersonic nozzle.

1.2 Laboratory unit description

Working area of the unit for given laboratory work represents vertically plane unshaped (with straight generatrix of profile) supersonic nozzle, which is connected to pipe line of all vacuum system through the feed valve.

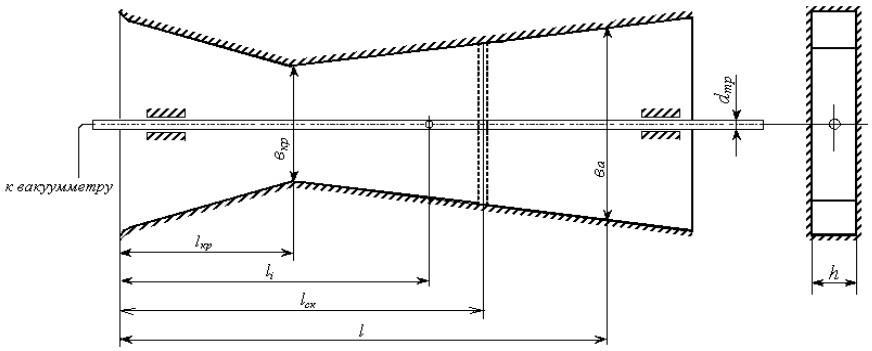

Fig. 3. Unit working area scheme

Air flow motion is caused by the pressure difference between atmosphere pressure $p_н$ on the entrance and low negative pressure $p_{пр}$, created by the vacuum pump. Pressure difference in the nozzle change (change of the air flow regimes) is executed by feed valve in the tube line. The tube with diameter d=1.5 mm is placed inside the nozzle along the axis. For static pressure of the air flow measurement, on the side surface of the tube the orifice with diameter d = 0,4 mm is placed. One end of the tube (backward) is closed and the front end is connected with vacuum gauge. Tube orifice location is fixed by finger connected with tube on the external surface of the nozzle wall. The displacement of the tube with side orifice is carried out by screw and allow measurement of the static pressure in any nozzle section. Minimal section of the nozzle is placed on the l=20 mm distance from the entrance and calculated section on the exit (sect. a) on the distance l=60 mm from the critical. Common nozzle length is l = 80 mm. Nozzle thickness h = 6 mm. Nozzle width in the narrow section s_y = 9 mm, in the nozzle exit section s_a = 13 mm, in the section 0 on the entrance s_0 = 36 mm.

1.3 Work sequencing

1. The protocol for devices measurement recording and calculation results is prepared.

2. Air temperature $t_н$ and pressure $p_н$ in the classroom are measured.

3. Vacuum pump is turned on.

4, Laboratory unit is checked. The tube inside the nozzle must be located so, that centre of its side orifice matches with nozzle entrance section, where l = 0.

5. Unit feed valve is smoothly opened.

6. The negative pressure after the nozzle $p_{вак}^{пр}$ is measured.

7. Air flow static pressure is measured in the sections, pointed in the protocol. For this purpose, by the screw rotation, tube orifice is moved inside the nozzle according to the section coordinates.

8. The negative pressure after the nozzle is increased by smooth closing of the feed valve and checking the condition that static pressure in the minimal section zone must remains the same.

9. Paragraphs 4, 6 and 7 are repeated for steady supersonic flow.

Experimental protocol example

Measured values																
Supersonic regime 1, p_{vac}^{neg} = div.																
№ sec	1	2	3	4	5	6	7	8	9	10	11	12	13	14	15	16
l, mm	5	10	15	17,5	20	22,5	25	27,5	30	32,5	35	37,5	40	50	60	80
p_{vac}, div																
Supersonic regime 2, p_{vac}^{neg} = div.																
p_{vac}, div																
Subsonic regime, p_{vac}^{neg} = div.																
p_{vac}, div																
Calculated values																
Supersonic regime 1, $p_{пр}$= kPa, $p_{neg}/p_н$=																
p, kPa																
c, m/sec																
G_c, kg/sec																
Supersonic regime 2, $p_{пр}$= kPa , $p_{neg}/p_н$=																
p, kPa																
c, m/sec																
G_c, kg/sec																
Subsonic regime , $p_{пр}$= kPa , $p_{neg}/p_н$=																
p, kPa																
c, m/sec																
G_c, kg/sec																

10. The negative pressure after the nozzle is increased by smooth closing of the feed valve and checking the condition that static pressure in the minimal section zone decreases.

11. Paragraphs 4, 6 and 7 are repeated for steady subsonic flow.

12. Vacuum pump is turned off.

13. The results of the measurements are recorded to protocol.

1.4 Data reduction process

1. Stagnation temperature T^* and critical velocity c_{cr} by expression (1.5) in all sections of the air flow along the axis on all regimes are calculated

$$T^* = t_н + 273,$$

where $t_н$ is measured atmosphere air temperature in Celsius, for air $\kappa = 1{,}4$; $R = 287$ J/kg K.

2. Absolute static pressure p is determined by the results of the measurements in air flow sections along the nozzle axis for all regimes

$$p = p_н - p_{vac} = p_н - p_{vac,\,div}\, n,$$

where $p_н$ is air atmosphere pressure;

n is division value (kPa) of the standard gauge.

3. Location of the shock wave is determined in the nozzle on supersonic regimes, i.e. l_{sw1} and l_{sw2}, by the character of static pressure p changing along the nozzle axis.

4. Air flow velocity is calculated by (1.6) expression in section prior shock wave neglecting friction losses, when $p^*i = p_н = const$, for two supersonic regimes.

Similar calculations are carried out in all flow sections on subsonic regime.

5. Stagnation pressure p^* after shock wave is determined on expression (1.7) on supersonic regimes.

6. Air flow velocity c in sections after the shock wave is calculated by expression (1.6) in section after the shock wave neglecting friction losses, when $p_i^* = p_{aft}^* = const$, for two supersonic regimes.

7. Mass flow rate in the entrance section 1 of the nozzle is calculated for all regimes

$$G_c = \rho_1 c_1 S_1 = m_G S_1 \frac{p_1}{\sqrt{T_1^*}} y(\lambda_1),$$

where $m_G = \sqrt{\left(\frac{2}{\kappa+1}\right)^{\frac{\kappa+1}{\kappa-1}} \cdot \frac{\kappa}{R}}$;

for air $\kappa = 1{,}4$; $R = 287$ J/kg K, $m_G = 0{,}0404 \frac{\sec \cdot K^{1/2}}{m}$;

$$y(\lambda_1) = \left(\frac{\kappa+1}{2}\right)^{\frac{1}{\kappa-1}} \cdot \lambda_1 \Big/ \left(1 - \frac{\kappa-1}{\kappa+1}\lambda_1^2\right); \quad \lambda_1 = \frac{c_1}{a_{cr}};$$

$S_1 = b_1 h$ - entrance section 1 of the plane nozzle, $S_1 = 31{,}5 \cdot 6 \cdot 10^{-6} = 189 \cdot 10^{-6}$, м^2.

8. The results of the calculation are recorded into the protocol and curves of the p, c, a_{cr} changing along the nozzle length l are plotted for all regimes and also G_c change vs pressure relation $\frac{p_{пр}}{p_н}$.

1.5 Report content

1. Experiment protocol with unit working area scheme.

2. Curves of the static pressure p change along the nozzle length l for all regimes.

3. Curves of the velocity c and critical velocity $c_{cr} = a_{cr}$ change along the nozzle length l for all regimes.

4. Curve of the mass flow rate change vs pressure relation $\frac{p_{пр}}{p_н}$ for all regimes.

5. Comparison of the experiment results. Determination of the shock wave location change vs pressure relation $\frac{p_{пр}}{p_н}$ on supersonic regimes.

6. Conclusions.

1.6 Test questions.

1. Why does the air flow in Laval nozzle can be considered as energetically insulated?

2. Which forces cause flow acceleration in Laval nozzle?

3. Which energy conversation occurs in the Laval nozzle on different nozzle regimes?

4. What condition required for stagnation pressure be the same for entire flow?

5. How to determine the stagnation pressure in entrance and narrow nozzle section by using experimental results?

6. How to determine the stagnation pressure losses in shock wave by using experimental results?

7. Why does flow in the Laval nozzle became critical in some section after the narrow nozzle section?

8. What condition is needed for flow to be critical in narrow section?

9. Why does shock wave moves to narrow section of the Laval nozzle with increasing of the negative pressure?

10. In what direction does shock wave will move with increasing or decreasing of the stagnation pressure of the flow prior Laval nozzle with constant negative pressure after the nozzle?

11. What is flow pressure on the exit from the Laval nozzle during nozzle work with shock wave presence inside the nozzle?

1.7 Reference literature

1. Abramovich G.N. Applied gas dynamics. Nauka. 1991.

2. Sergel O. S. Applied hydrogasdynamic. Nauka. 1981.

3. Lojcjanskij L.G. Fluid mechanics. Nauka. 1987.

Chapter 2. Supersonic flow around cylinder

The purpose of the work is comparison of the stream patterns of flow around cylinder (cylinder tube) by real (viscous) and potential plane subsonic air flows by comparison of the their pressure distribution along the cylinder perimeter. Another purpose is studying of body resistance estimation method by using resistance coefficient and experimental determination of this coefficient value and pressure and velocity change along subsonic and supersonic flows with solid body (cylinder) placement in them.

2.1 Theoretical basis of the experiment

Potential motion is non-vortex motion where angular velocity components of the fluid particles in relation to the centre of rotation, i.e. ω_x, ω_y, ω_z, vortex components in any point of flow are equal to 0. Potential motion takes place in case of ideal fluid (gas). However, studying of this motion has significant influence during tasks of flow around body by real (viscous) fluids solving.

Two-dimensional parallel flow with steady potential flow of incompressible fluid is presented on fig. 2.1.

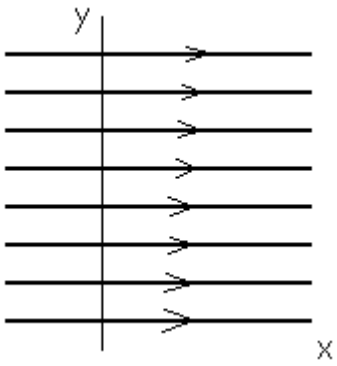

Fig. 2.1 Two-dimensional parallel flow

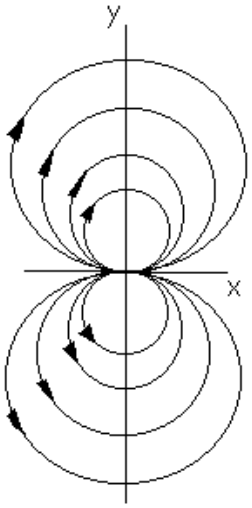

Fig. 2.2 Planar dipole stream lines

Dipole is a flow which appear if source and drain of equal flow rates are applied. Planar dipole stream lines represent circles of same radiuses, passing through start of coordinate system, which have centers on the y axes (fig. 2.2).

From the theoretical hydromechanics it is known that stream patter of flow around cylinder by two-dimensional parallel flow can be obtain by applying of two-dimensional parallel flow to dipole. Stream lines of resulted flows are cubic curves (fig. 2.3).

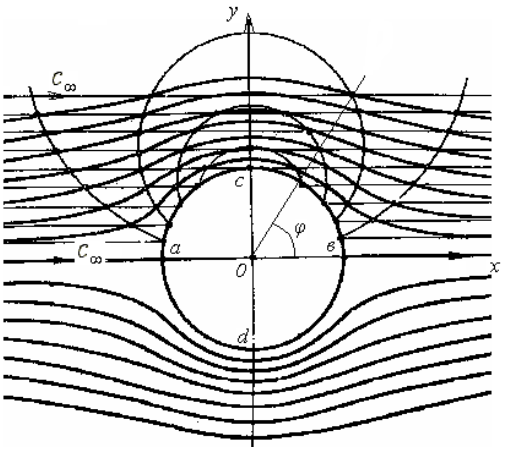

Fig. 2.3. Stream pattern of the flow around cylinder by plane potential flow of incompressible fluid.

Since during the flow around solid bodies by potential non-viscous flow of fluid , velocities on the body surface in each point are directed tangentially to the flowed circuit, any stream line of resulted flow can be considered as solid body boundary. Stream pattern of different solid bodies can be obtained. Considering stream line. which is circle, as a solid body boundary, we get stream pattern of the

flow around circle cylinder. In this case, velocity components for any point on the flowed cylinder surface in polar coordinate system are equal to c_r=0; $c_\varphi = -2c_\infty sin\varphi$. So, velocity on the cylinder surface depends only on approach flow velocity c_∞ and φ angle and independent from the cylinder radius. It is equal to 0 in points *a* and *b* and is twice as approach flow velocity in points *c* and *d* (fig. 2.3). In fluid flow, immediately bordering the cylinder, on the areas from a to c and from a to d, velocity continually increases in value from 0 to $2c_\infty$. Farther flow motion from c to b and from d to b takes place with deceleration to zero velocity in point b. If velocity distribution along the cylinder surface is known, pressure distribution can be obtained. For this purpose, Bernoulli integral is used, which is fair for all flow area of the incompressible fluid ($\rho = const$) without presence of viscosity and rotation of particles. Choosing on point of flow on infinity, where flow is undisturbed, with p_∞ and c_∞ parameters, and other point on the cylinder surface, we find

$$\frac{p}{\rho} + \frac{c^2}{2} = \frac{p_\infty}{\rho} + \frac{c_\infty^2}{2}$$

or

$$p - p_\infty = \frac{\rho \cdot c_\infty^2}{2}\left(1 - \frac{c^2}{c_\infty^2}\right).$$

$$p = p_\infty + \frac{\rho \cdot c_\infty^2}{2}\left(1 - 4\sin^2\varphi\right), \qquad (2.1)$$

because $c = -2c_\infty \sin\varphi$.

It should be taken into account that during the flow around cylinder by gas expression (1) is approximate because it doesn't takes gas density ρ change into account. However, during subsonic flow with Mach number $M_\infty \leq 0{,}3$ compressibility influence can be neglected.

From the symmetric pressure distribution along the cylinder it is followed that resulting flow pressure force acting to the cylinder is equal to 0, i.e. cylinder suffer neither resistance (projection of the resulting force on x axis) nor lift force (projection of the resulting force on y axis). This conclusion is rigorously proven

for the case of potential flow around body of arbitrary shape. It is Euler-d'Alembert paradox. This process of fluid flow around body seems paradoxical because in real case stream pattern of real fluid flow around body significantly differ from described case and solid body always resist to flows.

Contradiction with paradox is explained as in real flow assumption in the theoretical basis of the paradox are not accomplished.

Due to the viscosity, fluid velocity on the surface of the body will be equal to 0 and near the surface boundary layer takes place (fig. 2.4).

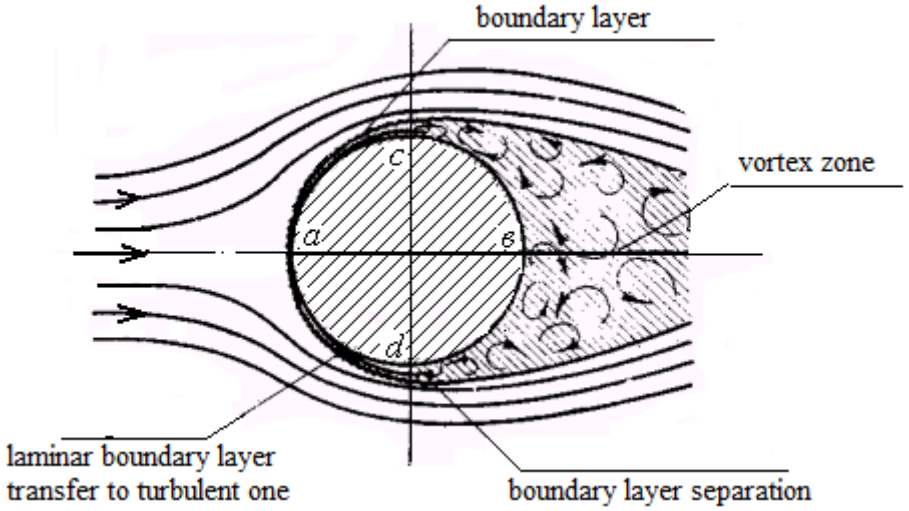

Fig. 2.4. Stream pattern of the real fluid flow around cylinder.

On cylinder front surface pressure gradient is negative (pressure decrease) and that's why boundary determining friction resistance layer here is thin and relatively weakly influence pressure distribution during potential flow (prior φ = $20\ldots30^0$ these distributions are nearly the same). Boundary layer thickness in the flow direction increases.

On the rear cylinder surface boundary layer development continues with positive pressure gradient (pressure increases). It lead to fast increasing of the boundary layer thickness and appearing of the reverse fluid particles motion which lose their kinetic energy due to viscosity. Boundary layer separation from the body is observed. After the separation place large vortexes and reverse streams take place and pressure on the surface of the cylinder doesn't change. So, viscosity presence causes not only friction resistance but also determines flow pattern which creates decreased pressure area after the cylinder. Pressure asymmetry causes

additional body resistance. The sum of the friction and pressure resistance is total or profile resistance of the streamlined body. if the body has smooth offsets (for example, airplane wind profile, compressor or turbine blades, carbody) and it is flown without flow separation, during the subsonic flow friction forces will be main part of the resistance. If body is badly shaped, i.e. sphere, cylinder or plate, mounted perpendicularly to flow, flow separation takes place, and to resistance, caused by friction, resistance, caused by pressure, is added. The last term can significantly exceed the first term.

During the real fluid flow around body lift force also appears. The task of lift force determination, appearing in case of plane potential flow around the profile, was successfully solved by Zhukovsky and Chaplygin. Zhukovsky theorem aboud wing lift force are the basis of wing theory and winged profiles, and also in theory of body profiling.

For analysis and experimental data use suitability non-dimensional coefficients are introduced, in which profile surface unit area values are related to velocity head of the approached flow. Reference area for circle cylinder is equal to product of cylinder width and its diameter d, i.e. $S_c = h \cdot d$, for sphere master cross-section area, i.e. $S_s = \pi \cdot d_s^2 / 4$, for blade profile unit – chord b, i.e. shortest distance between end points of profile.

So, pressure resistance coefficient during gas flow around circle cylinder is equal to

$$c_{x_p} = \frac{P_ц}{S \cdot (\rho_\infty \cdot c_\infty^2 / 2)}, \qquad (2)$$

where P_c is resulting gas flow pressure force in projection to axis x direction, i.e. pressure resistance force;

S – cylinder reference area, $S_ц = h \cdot d_ц$;

$\rho \cdot_\infty \cdot c_\infty^2 / 2$ - velocity head of the approached flow.

During the flow around cylinder tube by real plane supersonic flow shock wave, similar to direct shock wave, appears before the tube. After the direct shock wave flow became subsonic. In the shock wave zone stagnation pressure p^*

decrease and stagnation temperature T^* remains constant which is a property of the energetically insulated gas flow. Stagnation pressure decreasing in the shock wave is caused by entropy increase as a result of the irreversible process of kinetic energy converting to heat energy. Stagnation pressure losses are estimated by coefficient of the stagnation pressure change $\sigma = p^*_{aft} \Big/ p^*_{bef}$.

2.2 Laboratory unit description

Unit working area for given laboratory work is presented on fig. 5.

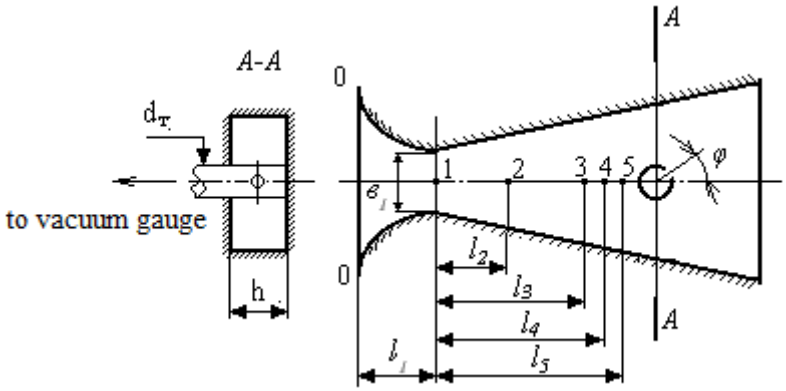

Fig. 5 Unit working area scheme

Air to the working area comes from the classroom atmosphere. Air flow motion is caused by the pressure difference between atmosphere pressure $p_н$ on the entrance and low negative pressure p_{np}, created by the vacuum pump. Pressure difference in the nozzle change (change of the air flow regimes) is executed by feed valve in the tube line.

In the expansion part of the narrowing-expansion nozzle, cylinder tube is mounted with diameter $d_т$ = 1,5 mm. There is an orifice with diameter d=0,3 mm for static pressure measurement of the surface of tube, streamed by flow, in section coincided with nozzle axis. One end of the tube (backward) is closed and the front end is connected with vacuum gauge. Due to the small tube diameter and considering its axis-symmetry, pressure measurement in different points of its perimeter is carried out not through the separate orifices but through one and the same orifice by rotation of the tube along its axis. Rotation angle φ is fixed by arrow on circle with angle scale, mounted on external side of the nozzle side surface. Indication of the φ is carried

out from the axis, coincide with nozzle axis, i.e. if $\varphi=0^0$ orifice is directed towards flow and measured pressure is equal to stagnation pressure (fig. 5). There are 5 drain orifices in sections 1…5 for air flow static pressure measurement. Flow pressure measurement are carried out by standard vacuum gauges of spring type. Distances between sections 1,2,3,4,5 and entrance of the nozzle are equal to l_1 = 25 mm, l_2 = 49mm, l_3 = 72mm, l_4 = 75 mm, l_5 = 79 mm correspondingly. Nozzle width h = 6 mm.

2.3 Work sequencing

1. The protocol for devices measurement recording and calculation results is prepared.

2. Air temperature $t_н$ and pressure $p_н$ in the classroom are measured.

3. Vacuum pump is turned on.

Experimental protocol example

Measured values													
Supersonic flow													
№sec	1	2	3	4	5								
p_{vac}, div													
Subsonic flow													
p_{vac}, div													
φ, deg	0	15	30	45	60	75	90	105	120	135	150	165	180
$p^{on}_{vac,\phi}$, div													
Calculated values													
Supersonic flow													
№sec.	1	2	3	4	5								
l, mm	25	49	72	75	79								
p, kPa													
p^*, kPa													
c, m/sec													
Subsonic flow													
p, kPa													
p^*, kPa													
c, m/sec													
p^{on}_{φ}, kPa													
p^{calc}_{ϕ}, kPa													

4. Laboratory unit is checked. The tube inside the nozzle must be located so, that arrow on the circle on the external side of the side nozzle wall was on zero position.

5. Unit feed valve is smoothly opened. Air flow in the nozzle corresponds to supersonic flow.

6. Measurements of the vacuum gauge, connected with receivers of static pressure in 5 sections of air flow along the nozzle, are recorded.

7.Measurement of the vacuum gauge, connected with cylinder tube in the nozzle with $\varphi = 0^0$ is recorded.

8. Subsonic air flow regime is set by smooth closing the feed valve until static pressure in section 1 start to change and became less, than on previous (supersonic) regime.

9. Paragraphs 6 and 7 are repeated for subsonic flow regime.

10. Without air flow regime changing static pressure on the surface of the cylinder tube is measured with φ angle values varies from 15^0 to 180^0 in increments of 15^0. Angle is fixed by arrow on the circle with angle scale.

11. Vacuum pump is turned off.

12. The results of the measurements are recorded to protocol.

2.4 Data reduction process

1. Stagnation temperature $T,^*$ similar in all sections of the air flow along the axis on all regimes, are calculated

$$T^* = t_н + 273,$$

where $t_н$ is measured atmosphere air temperature in Celsius, for air $\kappa = 1{,}4$; $R = 287$ J/kg K.

2. Absolute static pressure p is determined by the results of the measurements in air flow sections along the nozzle axis for all regimes

$$p = p_н - p_{vac} = p_н - p_{vac,\,div}\, n,$$

where $p_н$ is air atmosphere pressure;

n is division value (kPa) of the standard gauge.

3. Absolute pressure on the cylinder tube surface with φ angle values vary from 0 to 180^0 during the subsonic air real flow

$$p^{on}_{\varphi} = p_н - p_{vac\varphi} = p_н - p_{vac\varphi,\ div} \cdot n,$$

where $p_н$ is air atmosphere pressure;

n is division value (kPa) of the standard gauge.

4. Stagnation pressure p^* in sections 1…5 for two regimes is determined by accepting the linear dependency of its change along the nozzle length from atmosphere pressure p to $p^* = p^{on}_{\varphi=0^0}$ in flow section prior to cylinder tube.

5. Air velocity c_{mean} is calculated in 5 sections of the flow for two regimes

$$c_{cp} = \sqrt{\frac{2\kappa}{\kappa - 1} RT^* \left[1 - \left(\frac{p}{p^*}\right)^{\frac{\kappa-1}{\kappa}}\right]}$$

where k = 1,4; R = 287 J/kg K for air.

6. Air flow critical velocity c_{cr}, similar in all flow sections along the nozzle axis, is determined for two regimes

$$c_{cr} = a_{cr} = \sqrt{\frac{2\kappa}{\kappa + 1} R T^*},$$

where $T^* = T_н$ is stagnation temperature.

7. Location of the direct shock wave l is determined in the nozzle on supersonic regimes, by the character of static pressure p changing along the nozzle axis.

8. Coefficient of stagnation pressure change in direct shock wave is determined

$$\sigma_{dsw} = \frac{p^*_{bef}}{p^*_{aft}}$$

where p^*_{bef} is air stagnation pressure in section before the shock wave, $p^*_{aft} = p^{on}_{\varphi=0}$ is air pressure on the cylinder tube surface with $\varphi=0^0$.

9. Coefficient of stagnation pressure change in direct shock wave is determined by expression

$$G_{dsw} = \lambda_{bef}^2 \left[\frac{1 - \frac{\kappa - 1}{\kappa + 1} \cdot \lambda_{bef}^2}{1 - \frac{\kappa - 1}{\kappa + 1} \cdot \frac{1}{\lambda_{bef}^2}} \right]^{\frac{1}{\kappa - 1}}$$

where $\lambda_{bef} = c_{bef} / a_{cr}$ is relative air velocity in section before the shock wave.

10. Air density ρ_5 is determined in section 5 on subsonic regime, considering $p^*_5 = p_{\varphi=0}$,

$$\rho_5 = \varepsilon_{(\lambda)} \rho^*_5,$$

where $\rho^*_5 = \frac{p^*_5}{RT^*_5} = \frac{p_{\varphi=0^0}}{RT_н}$ - air density, determined by stagnation parameters.

$\varepsilon_{(\lambda)}$ is gas dynamic function, determined by expression

$$\varepsilon_\lambda = \left(1 - \frac{\kappa - 1}{\kappa + 1} \lambda_5^2\right)^{\frac{1}{\kappa - 1}}, \text{ where } \lambda_5 = \frac{c_5}{a_{cr}}.$$

11. Absolute pressure p_ϕ^{calc} on the cylinder tube surface with φ angle vales varies from 0 to 180^0 with increment of 15^0, considering unperturbed flow parameters equal in section 5, i.e. $p_\infty = p_5$, $\rho_\infty = \rho_5$, $c_\infty = c_5$, is determined by expression (2.1).

12. The force of air flow pressure on cylinder tube in projection on axis direction is calculated

$$P_ц = \frac{\pi \cdot dh}{24 \cdot 10^3} \left[\begin{array}{l} \left(p_\varphi^{on}\right)_0 \cdot \cos 0^0 + 2\left(p_\varphi^{on}\right)_{15} \cdot \cos 15^0 + \ldots \\ + 2\left(p_\varphi^{on}\right)_{165} \cdot \cos 165^0 + \left(p_\varphi^{on}\right)_{180} \cdot \cos 180^0 \end{array} \right]$$

where d – cylinder tube diameter,

h – width of the plane air flow around cylinder tube,

p_φ^{on} – measured absolute pressure of the air on the surface of the cylinder tube, corresponding to the determined value of angle φ.

13. Pressure resistance coefficient of the circle cylinder is calculated by expression (2.2) considering , $\rho_\infty = \rho_5$, $c_\infty = c_5$, , $S_c = 1{,}5 \cdot 6 \cdot 10^{-6} = 9 \cdot 10^{-6}$, m^2.

14. The results of the calculation are recorded to protocol. Curves of p и p^* change along the nozzle length l (sections 1…5) for two regimes and also dependencies of $p_{\varphi}^{оп}$ and $p_{\varphi}^{расч}$ on the angle φ in polar coordinate system are plotted.

2.5 Report content

1. Experiment protocol with unit working area scheme.

2. Curves of the static pressure p and stagnation pressure p^* change along the nozzle length l for all regimes.

3. Curves of the velocity c change along the nozzle length l for all regimes.

4. Pressure p_{φ} distribution curves along the tube perimeter during flow around tube by plane real and potential flows in polar coordinate system.

5. Comparison of the experiment values of the stagnation pressure change coefficient σ in direct shock wave.

6. Conclusions.

2.6 Test questions

1. What assumptions are in the basis of the Euler-d'Alembert paradox proof in fluid mechanics?

2. Why there assumptions are not appropriate during real (viscous) flow around bodies?

3. Why flow around the cylinder by non-vortex flow will be continuous and fully symmetric?

4. How do slight differences in pressure distributions on front cylinder surface during flow around it by real and potential flows are explained?

5. How does pressure resistance of the solid bodies during flow around it with and without flow separation explained?

6. How to check that, when feed valve is fully opened, subsonic regime of flow around cylinder is set?

7. Which value of the φ angle is necessary to pressure on cylinder surface to be the same as stagnation pressure of the flow?

8. What features of the stagnation pressure during the supersonic flow in comparison with subsonic one?

9. How to determined values of c, p, T, ρ, p^*, T^* with direct shock wave presence during flow around cylinder?

2.7 Reference literature

1. Abramovich G.N. Applied gas dynamics. Nauka. 1991.
2. Sergel O. S. Applied hydrogasdynamic. Nauka. 1981.
3. Lojcjanskij L.G. Fluid mechanics. Nauka. 1987.